Physics and Chemistry of the Earth xxx (2015) 1–10

Contents lists available at ScienceDirect

Physics and Chemistry of the Earth

journal homepage: www.elsevier.com/locate/pce

Spatial scale impact on daily surface water and sediment fluxes in Thukela river, South Africa

Macdex Mutema [a], Graham Jewitt [a], Pauline Chivenge [a, b], Samuel Kusangaya [a], Vincent Chaplot [a, c, *]

[a] CWRR, SAEES, University of KwaZulu-Natal, PB X01, Scottsville 3209, Pietermaritzburg, South Africa
[b] International Crops Research Institute for the Semi-Arid Tropics, P O Box 776, Bulawayo, Zimbabwe
[c] Institut de Recherche pour le Développement (IRD), Laboratoire d'Océanographie et du Climat (LOCEAN), Université Pierre et Marie Curie, 4, place Jussieu 75252 Paris Cedex 05, France

A R T I C L E I N F O

Article history:
Received 26 March 2015
Received in revised form
28 September 2015
Accepted 1 October 2015
Available online xxx

Keywords:
Erosion mechanisms
Multiple nested catchments
Sediment fluxes
Water quality

A B S T R A C T

The on- and off-site effects of soil erosion in many environments are well known, but there is still limited understanding of the fluxes in downstream direction due, among other factors, to scarce and poor quality. A four year study to (i) evaluate water and sediment fluxes at different spatio-temporal scales and (ii) interpret the results in terms of processes involved and the controlling factors, was conducted in Thukela basin, South Africa. Five hierarchically nested catchments; namely microcatchment (0.23 km^2), subcatchment (1.20 km^2), catchment (9.75 km^2), sub-basin (253 km^2) and basin (29,038 km^2), were used in addition to fifteen (1 m^2) microplots and ten (10 m^2) plots on five locations within the microcatchment. The results showed 19% decrease of unit-area runoff (q) from 3.1 L m^{-2} day^{-1} at microplot to 2.5 L m^{-2} day^{-1} at plot scale followed by steeper (56%) decrease at microcatchment scale. The q decreased in downstream direction to very low level ($q \leq 0.26$ L m^{-2} day^{-1}). The changes in q were accompanied by initial 1% increase of soil loss (SL) from 18.8 g m^{-2} day^{-1} at microplot to 19.1 g m^{-2} day^{-1} at plot scale. The SL also decreased sharply (by 39 fold) to 0.50 g m^{-2} day^{-1} at microcatchment scale, followed by further decrease in downstream direction. The decrease of q with spatial scale was attributed to infiltration losses, while initial increase of SL signified greater competence of sheet than splash erosion. The decrease of SL beyond the plot scale was attributed to redistribution of the soil on the hillslope and deposition on the stream channel upstream of the microcatchment outlet. Therefore, erosion control strategies focussing on the recovery of vegetation on the slope and stabilisation of gullies are recommended.

1. Introduction

Soil erosion is a natural process primarily driven by lateral movement of water on landscapes and involves three main stages; soil particle detachment, transportation and sedimentation (Kinnell, 2008). Accelerated soil erosion has been a serious problem in different parts of the world for many years with well documented on- and off-site effects. On-site, soil loss impacts on long-term sustainability of agriculture due to loss of topsoil and reduction of soil depth for plant growth and nutrient storage. Off-site, soil erosion affects water security and the associated ecosystem functions (Flugel et al., 2003), through pollution and siltation of reservoirs (Chihombori et al., 2013; Négrel et al., 2014). Water pollution has also contributed to escalation of water supply costs, due to expensive water treatment processes to make the water portable for domestic use in some environments. Soil erosion has other far reaching effects such as global warming because it exposes soil aggregate protected organic carbon to decomposition processes, thus accelerating green-house gas (e.g. CO_2) emissions (Lal, 2004).

In spite of advances in knowledge on erosion mechanisms, there is no consensus among researchers on the scale effect on soil erosion fluxes on landscapes and stream channels. Several studies have reported on decreasing unit-area soil loss (SL) with landscape area or slope length (e.g. Van de Giesen et al., 2000; De Vente and Poesen, 2005; de Vente et al., 2007; Mayor et al., 2011). However,

* Corresponding author. Institut de Recherche pour le Développement (IRD), Laboratoire d'Océanographie et du Climat (LOCEAN), Université Pierre et Marie Curie, 4, place Jussieu, 75252 Paris Cedex 05, France.
E-mail addresses: chaplot@ird.fr, vincent.chaplot@gmail.com (V. Chaplot).

http://dx.doi.org/10.1016/j.pce.2015.10.001
1474-7065/© 2015 Published by Elsevier Ltd.

other studies (e.g. Le Bissonnais et al., 1998; Parsons et al., 2006) have reported on an initial increase of SL followed by a decrease with further increase of slope length. For example, Parsons et al. (2006) observed increasing SL up to a maximum at a slope length of 7 m and a decrease thereafter. Erosion studies have also reported on preferential removal and transport of certain soil particle size classes depending on spatio-temporal scale; however no consensus on particle sizes to be eroded at a particular scale exists. For example, Smith and Dragovich (2007) reported on selectivity for fine particles at small spatial areas while Shi et al. (2012) reported dominance by coarse materials. Soil erosion itself is a complex process dependent on interactions amongst many promoters like hydrological regimes (e.g. rainfall and surface flow), anthropogenic activities (e.g. land use and management), biotic (e.g. fauna and flora) and abiotic (e.g. soil properties and other non-living parameters) factors. General surface hydrology highlights a progression of soil erosion mechanisms from splash effect at point scale, lateral sheet and interrill at field level, to linear rill and gully mechanisms

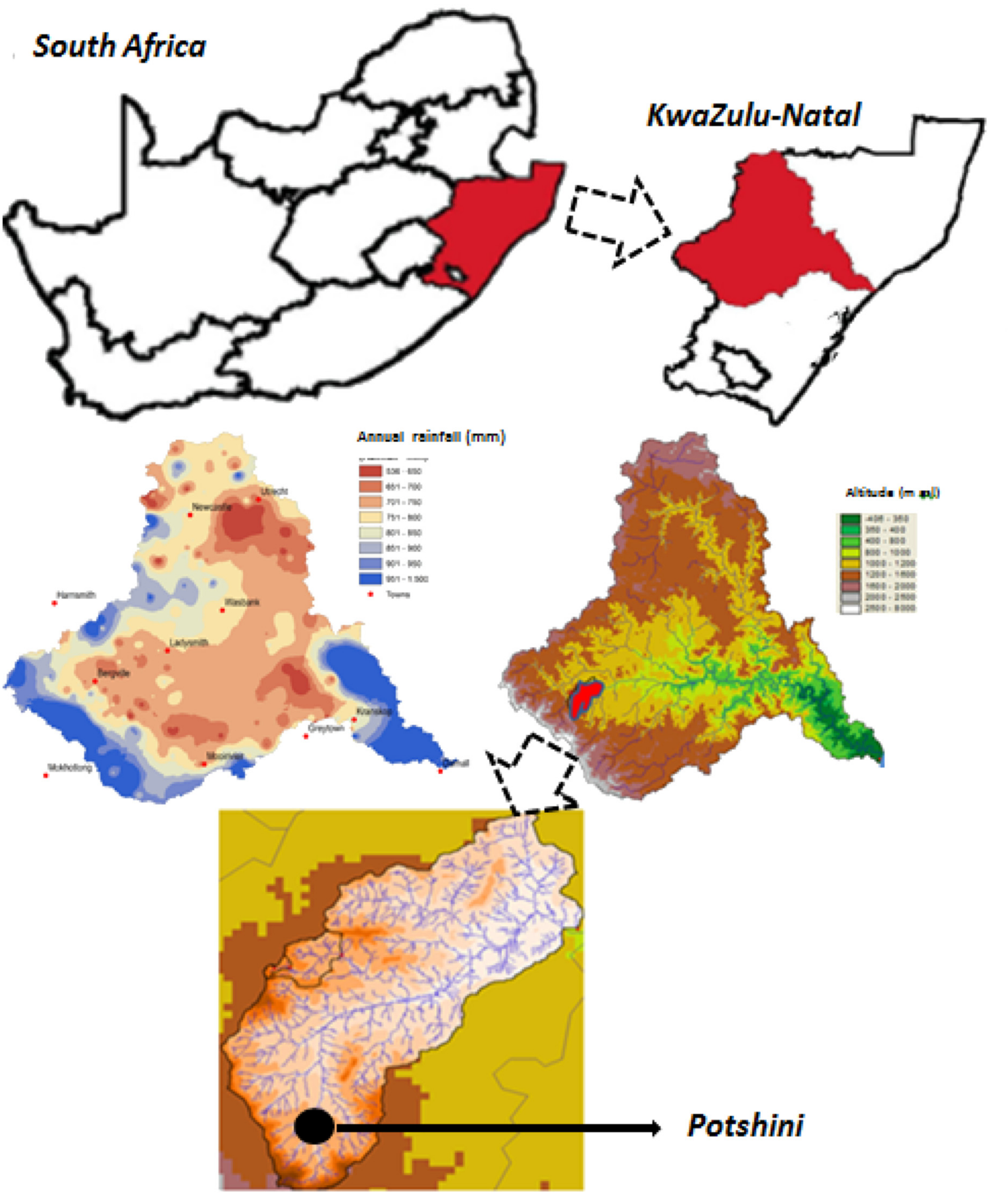

Fig. 1. Combo map showing the location of KwaZulu-Natal province within South Africa, the Thukela Basin in KwaZulu-Natal as well as the sub-basin in where Potshini catchment is located. Also shown are the annual rainfall (mm yr^{-1}) and altitude (masl) distribution maps of the Thukela Basin.

Please cite this article in press as: Mutema, M., et al., Spatial scale impact on daily surface water and sediment fluxes in Thukela river, South Africa, Physics and Chemistry of the Earth (2015), http://dx.doi.org/10.1016/j.pce.2015.10.001

at larger landscapes. This transition of mechanisms follows progress in channelization of surface flow and increasing competence to transport detached materials.

A four year (2010–2014) study was performed in Thukela Basin, South Africa, to (i) evaluate water and sediment fluxes at different spatio-temporal scales, and (ii) and interpret the results in terms of main processes involved and factors of control. Such a study is essential because river basin management aiming to reduce land degradation, improve water security and safeguard ecosystem health requires better knowledge of upstream–downstream changes in water and sediment fluxes.

2. Materials and methods

2.1. Study basin and experimental set-up

The study was carried out in Thukela Basin (28.97–31.43° E, 27.42–29.40° S), which is the largest river basin of KwaZulu-Natal province, South Africa, with approximate area of 30,000 km^2 (Fig. 1). The main river flows 502 km in an easterly direction from Drakensburg Mountains to the Indian Ocean. The basin climate varies from being largely subtropical in the high altitude zone to semi-arid in the valley region. Annual rainfall varies widely across the basin and from one year to the other; however most of the rain falls during summer months between September and April.

Progressively nested catchments; namely microcatchment (size 0.23 km^2), subcatchment (1.20 km^2), catchment (9.75 km^2), sub-basin (253 km^2) and basin (29,038 km^2), were used in this study. The microcatchment and subcatchment outlet were located in Potshini, a rural community 10 km west of Bergville town. The climate of Potshini was classified as sub-tropical with long-term annual rainfall, temperature and potential evaporation of 684 mm, 13 °C and 1600 mm, respectively (Schulze, 1997). The catchment and sub-basin outlets were located in a commercial farming zone. The basin outlet for the study was near Mandini (31.39°E, 29.14°S), about 1 km^2 upstream of Thukela mouth. In addition, fifteen runoff microplots (size 1 m^2) and 10 plots (10 m^2) replicated three and two times respectively on five hillslope positions within the microcatchment were used. The slope positions represented different levels of overgrazing in terms of vegetation cover (the microcatchment was used for communal livestock grazing), topography, soil types, geology and soil surface characteristics (Dlamini et al., 2011; Oakes et al., 2012; Orchard et al. 2013). The hillslope is very steep (50–70% gradient) with a relatively flat plateau. The main soil types here were reddish dolerites (of good drainage) extending from the plateau to a terrace downslope followed by *Acrisols* which were shallow at the mid-slope and deep (~2 m) at the bottom (Deckers et al., 1998). The topo-sequence on this slope suggested a full complement of recharge, interflow and responsive soils (Van Tol et al., 2013).

2.2. Equipment and measurements of water and sediment fluxes

2.2.1. Runoff microplots and plots

Each runoff microplot and plot was demarcated by galvanised metal sheets inserted 10 cm into the ground and leaving another 10 cm above ground to eliminate run-on water during rain events. Surface water and sediments generated collected into a protected gutter through openings in a downslope side metal sheet. The gutter was fitted with a delivery pipe connected to a reservoir about 1.5 m downslope. All runoff and sediments from microplots were collected into reservoirs. However, fractions of runoff and sediments had to be from plots to avoid frequent overtopping of reservoirs. One plot at each of the five slope positions was equipped with a water divisor to split flow into five parts and only one part was collected into the reservoir. The other plot was equipped with a tipping-bucket in addition to the divisor; hence one tenth of flow (and sediments) was collected into the reservoir. Accordingly, total flow and sediments from plots were obtained by multiplying measured quantities by five or ten.

2.2.2. Outlets on the stream channel

The equipment setup at microcatchment and subcatchment outlets was described in detail by Kongo et al. (2010). At each of the two outlets was an H-flume equipped with a differential pressure transducer (for continuous monitoring of stream stage) and automatic sampler (ISCO Model 2900). Both the pressure transducer and sampler were coupled to datalogger (CR200). The pressure transducer automatically converted stream stage to discharge (Q, L s^{-1}). The sampler was calibrated to collect water samples more frequently during high than low flows. The catchment outlet was a double-opening bridge culvert equipped with a pressure transducer. Another bridge culvert with eight holes marked the sub-basin outlet and flow measurements were done manually during weekly visits. Flow data at the basin outlet was obtained from the Department of Water Affairs online database. Water sampling at catchment, sub-basin and basin outlet was by hand from streamflow during visits. In addition to automatic samples, grab samples were collected during visits at micro- and subcatchment outlets.

A portable turbid-meter (TSS Portable HACH) was used to measure sediment concentration (SC, g L^{-1}) in water samples after

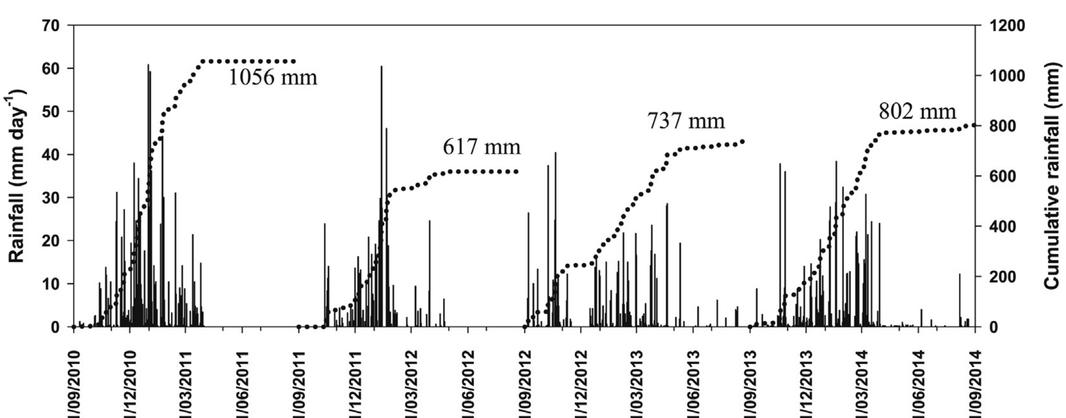

Fig. 2. Variability of rainfall (mm day^{-1}) and cumulative annual rainfalls for each of the years (mm yr^{-1}) during the study period as recorded by a tipping-bucket rain gauge at Potshini, South Africa.

Please cite this article in press as: Mutema, M., et al., Spatial scale impact on daily surface water and sediment fluxes in Thukela river, South Africa, Physics and Chemistry of the Earth (2015), http://dx.doi.org/10.1016/j.pce.2015.10.001

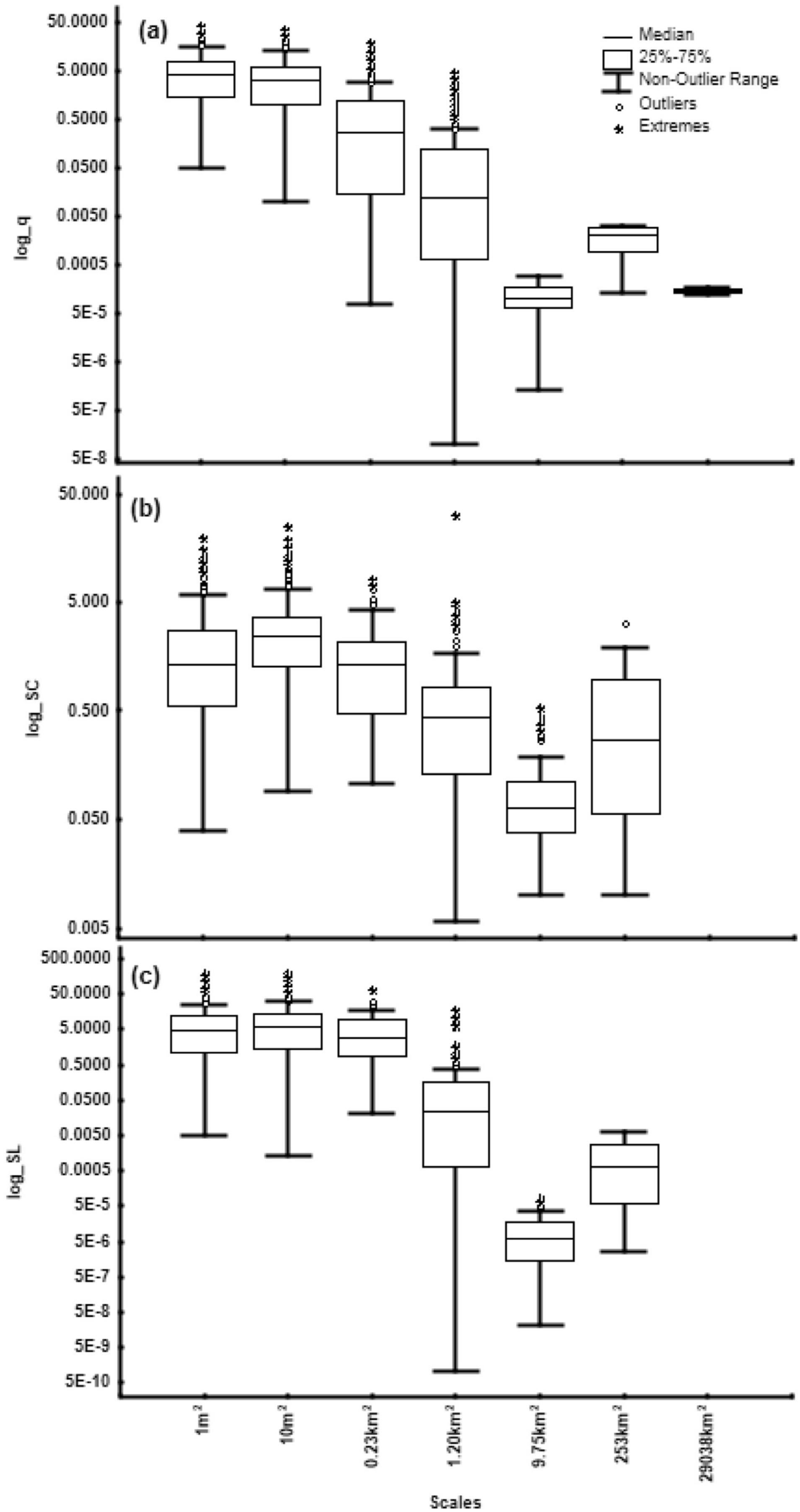

Fig. 3. Box plots showing medians, 25–75% and non-outlier ranges of (a) q: unit-area runoff (L m^{-2} day^{-1}), (b) SC: sediment concentrations (g L^{-1}), and (c) SL: soil losses (g m^{-2} day^{-1}) at different spatial scales (microplot: 1 m^2, plot: 10 m^2, microcatchment: 0.23 km^2, subcatchment: 1.20 km^2, catchment: 9.75 km^2, sub-basin: 253 km^2, and basin: 29,038 km^2) in Thukela basin during the study.

thorough stirring to obtain homogeneous water-sediment mixtures. Rainfall was measured by means of a tipping-bucket rain gauge located at Potshini. The rain gauge was connected to a data logger (CR200) and data collected was used to characterize the rain events in terms of total daily rainfall amount (Rainfall, mm day^{-1}), storm event duration (Dur, mins), average storm intensity (I, mm h^{-1}) and maximum 6-min rainfall intensity ($Max_{6min}I$, mm h^{-1}). Antecedent 3-day rainfall (PreRain-3, mm) and cumulative rainfall since the onset of the main rain season (RainC, mm) were also computed from the data.

2.3. Evaluation of daily water and sediment fluxes

Average runoff volume per day for the 15 microplots and 10 plots on the hillslope were divided by respective scale size to obtain a unit-area runoff flux (q, L m^{-2} day^{-1}). Discharge (Q, L s^{-1}) at stream outlets were added together to get daily values which were then divided by respective scale size (in m^2) to obtain unit-area runoff fluxes (q, L m^{-2} day^{-1}). The assumption here was that each m^2 within a scale size contributed uniformly to measured (or observed) runoff or surface flow. Simple linear interpolation was used to estimate daily q for day with no data (due to equipment failure or lack of measurement e.g. at sub-basin level). Average SC (g L^{-1}) for each day at the different scales was computed. Linear interpolation was also used to estimate SC for days without observed data. Soil loss fluxes (SL), the amount of sediment discharged per unit area per day, were calculated using the following equation (1).

$$SL = q \times SC \quad (1)$$

Where SL = soil loss flux (g m^{-2} day^{-1}), q = unit-area surface runoff flux (L m^{-2} day^{-1}) and SC = average sediment concentration (g L^{-1}).

2.3.1. Statistical analysis

Basic descriptive statistics of unit-area runoff (q), sediment concentrations (SC) and soil losses (SL) such as Min: minimum, Max: maximum, Median, Mean, Q1: quartile 1, Q2: quartile 2, Stdev: standard deviation, SE: standard error of mean, Skew: skewness, Kurt: Kurtosis and CV%: coefficient of variation were computed. Spearman rank correlation analysis was also performed to understand the one-on-one relationships between the fluxes and rainfall characteristics. Spearman coefficients were used because the Skewness and Kurtosis values (from the general statistics) indicated that the datasets were not normally distributed. In all analyses, differences and correlations were considered to be significant at $p < 0.05$, unless stated.

3. Results

3.1. Daily and annual rainfall during the study

Daily and annual rainfalls as recorded by the tipping-bucket rain gauge at Potshini during the study are presented in Fig. 2. The results show great variability of rainfall, from one year to the other. The highest annual rainfall (1056 mm yr^{-1}) was recorded in the first year of study and this was extremely wet in comparison with the long-term mean of nearby Bergville (684 mm yr^{-1}). However, this was followed by a dry year with annual rainfall of 617 mm yr^{-1}. The two remaining years were wetter than the long-term mean. Overall, the study period was wetter than average with a four-year mean annual rainfall of 807 mm yr^{-1}.

3.2. Variability of daily water and sediment fluxes with spatial scale

The box-plot results shown in Fig. 3 highlight the overall variability of unit-area runoff (Fig. 3a), sediment concentration (Fig. 3b) and soil losses (Fig. 3c) with spatial scale. The results in Fig. 3a show a decline of unit-area runoff (q) from microplot to plot scale followed by steeper decrease on the stream channel. On average, q decreased by 19% from 5.67 L m^{-2} day^{-1} at microplot to 4.59 L m^{-2} day^{-1} at plot scale (Table 1). This was followed by a 76% decrease from plot to 1.11 L m^{-2} day^{-1} at microcatchment scale. The q decreased further in a downstream direction, by 77% from microcatchment to subcatchment scale, and to very low values at catchment, sub-basin and basin scales. The decrease of q from microplot to plot scale was accompanied by increasing sediment concentration (SC) and unit-area soil losses (SL) (Fig. 3b–c). On

Table 1
General statistics of daily fluxes (q: unit-area runoff, SC: sediment concentration, and SL: soil loss) at different spatial scales (microplot: 1 m^2, plot: 10 m^2, microcatchment: 0.23 km^2, subcatchment: 1.20 km^2, catchment: 9.75 km^2, sub-basin: 253 km^2, and basin: 29,038 km^2) in Thukela basin during the study.

Scale	Min	Max	Median	Mean	Q1	Q3	Stdev	SE	Skew	Kurt	CV%
q (L m^{-2} day^{-1})											
$1m^2$	0.05	40.55	4.14	5.67	1.45	7.51	6.17	0.38	2.3	7.3	109
$10m^2$	0.01	36.31	3.25	4.59	1.00	6.02	5.19	0.32	2.4	8.4	113
0.23 km^2	8×10^{-5}	18.87	0.26	1.11	0.01	1.16	2.11	0.06	3.7	18.3	191
1.20 km^2	1×10^{-7}	4.69	0.01	0.26	6×10^{-5}	0.14	0.61	0.02	3.8	17.4	230
9.75 km^2	2×10^{-6}	3×10^{-5}	9×10^{-5}	1×10^{-4}	6×10^{-5}	2×10^{-5}	6×10^{-5}	2×10^{-6}	0.4	−0.3	65
253 km^2	1×10^{-4}	3×10^{-3}	2×10^{-4}	2×10^{-4}	9×10^{-5}	3×10^{-4}	1×10^{-4}	4×10^{-5}	−0.3	−1.3	50
29,038 km^2	1×10^{-4}	2×10^{-5}	2×10^{-5}	2×10^{-5}	1×10^{-5}	2×10^{-6}	1×10^{-5}	4×10^{-7}	−0.2	−1.2	9
SC (g L^{-1})											
$1m^2$	0.04	19.19	1.33	2.84	0.56	2.74	3.79	0.23	1.9	2.7	133
$10m^2$	0.09	24.35	2.45	3.77	1.28	3.60	4.23	0.26	1.9	3.2	112
0.23 km^2	0.01	7.94	0.01	0.14	0.01	0.01	0.64	0.02	7.1	61.5	450
1.20 km^2	0.01	4.93	0.01	0.08	0.01	0.01	0.38	0.01	8.1	73.6	487
9.75 km^2	0.01	0.53	0.01	0.02	0.01	0.01	0.04	1×10^{-4}	7.6	66.3	229
253 km^2	0.01	3.19	0.01	0.03	0.01	0.01	0.17	4×10^{-4}	10.4	132.4	531
SL (g m^{-2} day^{-1})											
$1m^2$	5×10^{-3}	778.03	4.97	34.19	1.12	14.14	83.46	5.17	4.4	27.1	244
$10m^2$	1×10^{-3}	884.07	6.57	34.70	1.53	15.65	85.91	5.32	5.4	41.0	248
0.23 km^2	8×10^{-7}	65.29	3×10^{-4}	0.50	1×10^{-5}	0.01	2.98	0.08	11.4	186.3	597
1.20 km^2	1×10^{-9}	17.22	2×10^{-5}	0.05	7×10^{-6}	2×10^{-4}	0.64	0.02	20.2	453.5	1338
9.75 km^2	1×10^{-8}	8×10^{-5}	1×10^{-6}	2×10^{-6}	7×10^{-7}	2×10^{-6}	7×10^{-6}	2×10^{-7}	8.0	73.5	293
253 km^2	1×10^{-6}	6×10^{-4}	2×10^{-5}	2×10^{-5}	1×10^{-5}	3×10^{-5}	7×10^{-5}	3×10^{-5}	6.0	39.4	434

Please cite this article in press as: Mutema, M., et al., Spatial scale impact on daily surface water and sediment fluxes in Thukela river, South Africa, Physics and Chemistry of the Earth (2015), http://dx.doi.org/10.1016/j.pce.2015.10.001

average, SC increased by 33% from 2.84 to 3.77 g L^{-1}, while SL increased by 1% only from 34.19 to 34.70 g m^{-2} day^{-1} (Table 1). This was followed by very sharp decrease of 96 and 99% for SC and SL respectively at microcatchment level. The rate of decrease in SL decrease between catchment outlets remained greater than that of SC in the downstream direction. For example, SC decreased by only 43% while SL decreased by 90% from microcatchment to sub-catchment outlet. The q, SC and SL results demonstrated greater magnitudes and dynamics within headwaters, especially the hillslope, than at greater spatial scales downstream. Therefore, further exploration of the fluxes would be more important in the headwaters (i.e. scales from microplot to catchment level) than the lower basin area.

3.3. Variability of daily water and sediment fluxes over time

The variability of q, SC and SL over time during the study period is shown in Figs. 4–6. The figures show that amplitudes of fluxes were greater with sharper peaks at microplot and plot scales; however the fluxes became more continuous and attenuated with increasing scale size. Despite being relatively dry (Fig. 2), the year 2011–2012 still recorded very high peaks of q, SC and SL at the hillslope scales (i.e. microplot to microcatchment). The winter rains recorded at Potshini in 2012–2013 and 2013–2014 (Fig. 2) did not

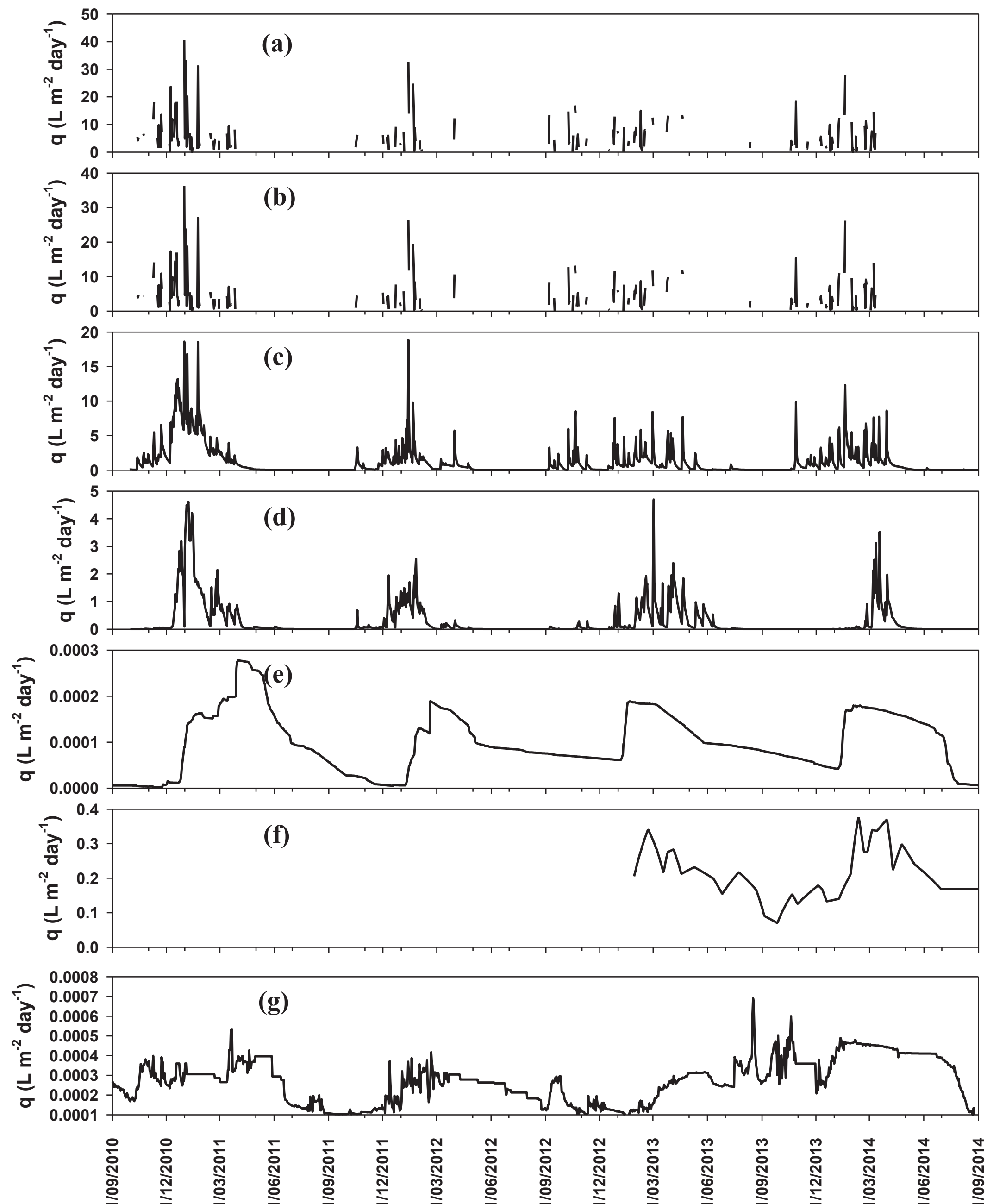

Fig. 4. Graphs showing variability of unit-area runoff fluxes (q, L m^{-2} day^{-1}) at (a) microplot, (b) plot, (c) microcatchment, (d) subcatchment, (e) catchment, (f) sub-basin and (g) basin scale in Thukela basin over time during the study period 2010–2014.

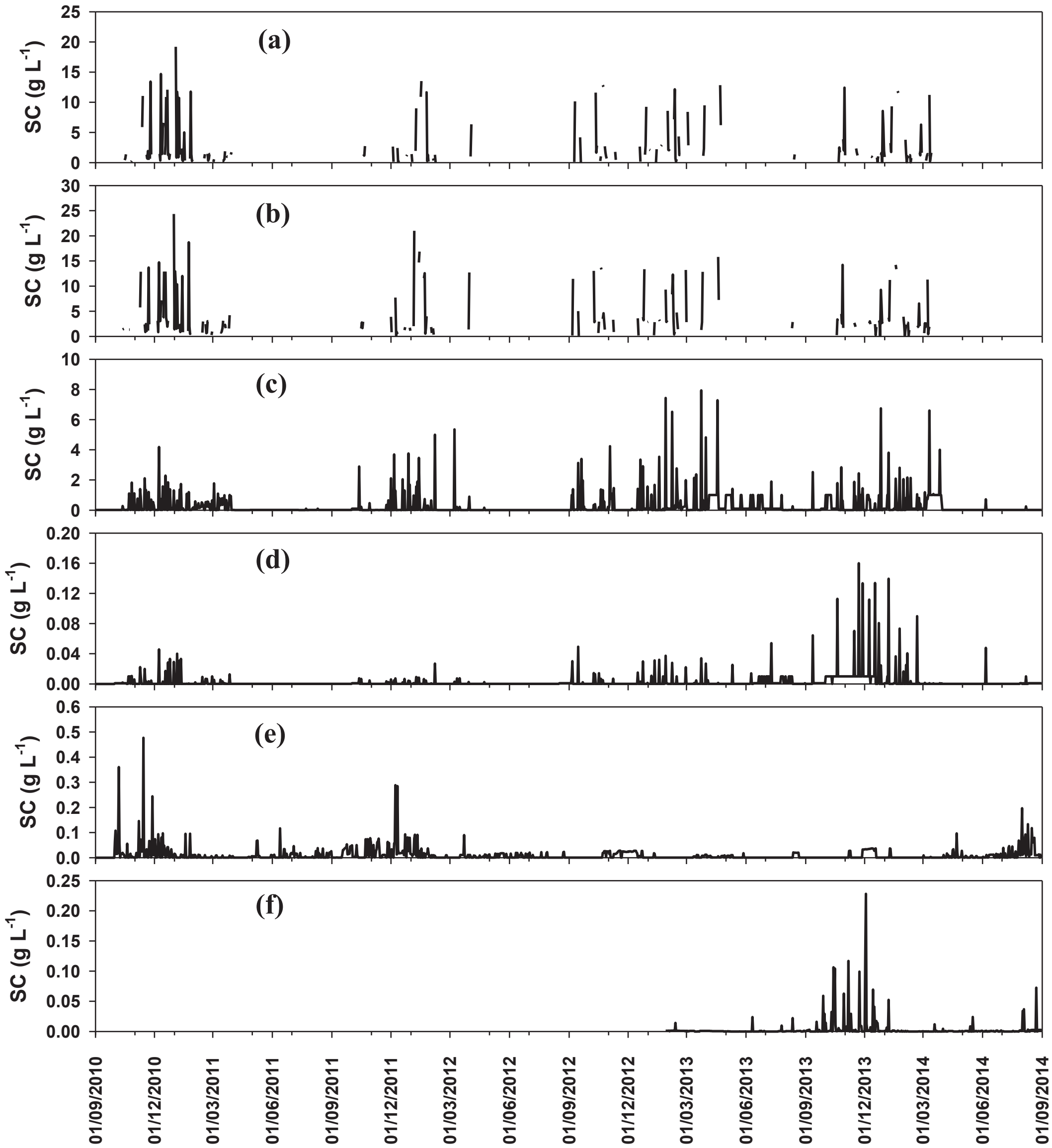

Fig. 5. Graphs showing variability of sediment concentrations (SC, g L^{-1}) at (a) microplot, (b) plot, (c) microcatchment, (d) subcatchment, (e) catchment, and (f) sub-basin scale in Thukela basin over time during the study period 2010–2014.

have any significant effect on q, SC and SL at outlets on the stream channel (Fig. 4c–g, Fig. 5c–f and Fig. 6c–f). Fluxes at catchment outlet were negligible in comparison to other headwater scales due, most probably, to the effect of two dams immediately upstream of the outlet.

As expected, final cumulative q was greatest and least at each spatial scale in year with greatest and least annual rainfall, respectively (Table 2). However, in spite of less annual rainfall, the year 2012–2013 still had 7 and 1% greater cumulative q at microplot and plot scale respectively than in 2013–2014. The microcatchment scale exhibited greatest cumulative q in years when annual rainfall was greater than 800 mm yr^{-1}, but the annual q at microcatchment was less than at microplot in years when annual rainfall was less than 800 mm yr^{-1}. The difference of annual q between microplot and microcatchment was greatest in the wettest year. It was also apparent from the results that plot scale did not always have greater cumulative annual SL than microplot scale. For example, microplot had greater annual SL than plot scale in 2012–2013 where the respective values were 1889 and 1853 g m^2 yr^{-1} for microplot and plot scale, respectively (Table 2). It was also ironic that greater annual rainfall did not always produce greater annual SL. For example, the subcatchment level had 3 fold greater annual SL in 2012–2013 than 2013–2014, despite the fact that annual rainfall was lower in 2012–2013 than 2013–2014.

3.4. Factors controlling water and sediment fluxes

The Spearman correlation coefficients (r_s) shown in Table 3 indicate significant and positive correlations between the rainfall characteristics and fluxes at all scales in the headwater, except for q at the catchment outlet. Catchment scale q correlated significantly and positively with RainC only. The r_s between the rainfall characteristics and fluxes decreased with spatial scale. However, the trends of r_s for RainC were, again, exceptions. For instance, r_s between q and RainC showed an increase from local scales (i.e. microplot and plot) to microcatchment and then decreased to

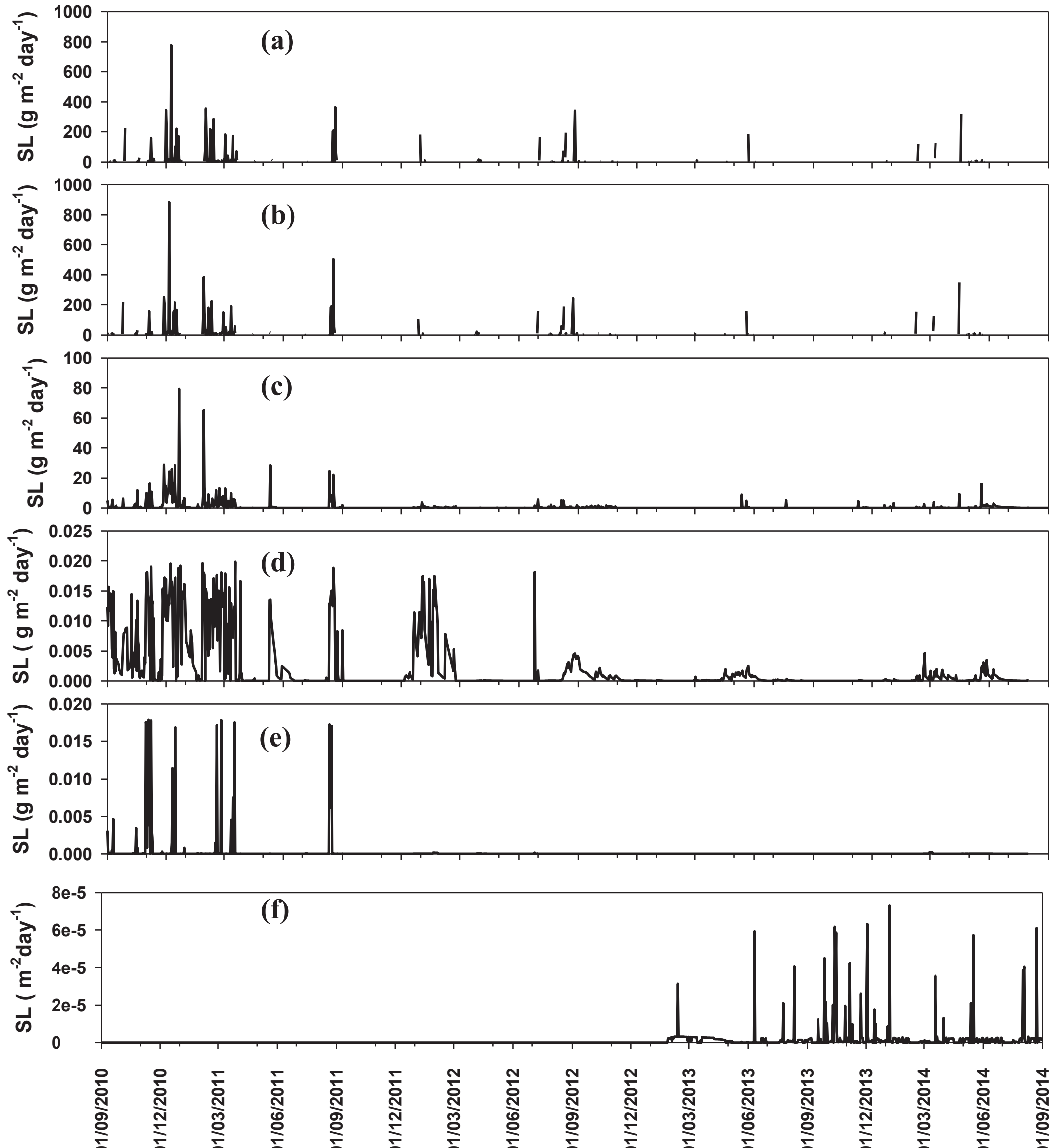

Fig. 6. Graphs showing variability of unit-area soil loss fluxes (SL, g m^{-2} day^{-1}) at (a) microplot, (b) plot, (c) microcatchment, (d) subcatchment, (e) catchment, and (f) sub-basin scale in Thukela basin over time during the study period 2010–2014.

catchment through the subcatchment level. A similar trend of r_s was shown between RainC and SL; however the r_s between RainC and SC decreased from local scales to microcatchment and then increased to catchment through the subcatchment level.

4. Discussion

The study results showed a general decrease of unit-area runoff with scale size (Table 1, Fig. 3a), which has also been widely reported in other studies (e.g. Van de Giesen et al., 2000; Joel et al., 2002; Asadzadeh et al., 2012; Thomaz and Vestena, 2012). This decrease of unit-area runoff with increasing area was mainly attributed to infiltration losses on hillslopes and stream channels. The infiltration losses increase with increasing surface area of contact and/or contact time; hence less surface flow volume per unit-area is expected to reach a designated outlet when these two increase. Greater infiltration on hillslopes, where flow is not fully channelized, is mainly promoted by physical barriers, such as vegetation patches, (Cammeraat, 2004; Mayor et al., 2011), which retard flow velocity thereby increasing the contact time between flow and the infiltrating surface. Even when flow channelizes, Dunkerley (2010) explained that channel-associated plants may still modify flow conditions, thus reducing flow speeds and flow competence. The much lower runoff fluxes at outlets along the stream channel than hillslope scales (Fig. 3a), suggested further streamflow losses to infiltration in a downstream direction. Semi-arid streams are generally dominated infiltration losses of streamflow (Sorman and Abdulrazzak, 1993). The wider variability of the runoff fluxes at microcatchment and subcatchment than at catchment and other downstream outlets signified incidences of rapid storm-flows whose peaks attenuate with increasing stream channel length due to increasing flow resistance and impoundments. The existence of two dams immediately upstream of the catchment outlet may also explain the very low runoff fluxes observed.

The increase of sediment concentration and unit-area soil losses

Table 2
Annual cumulative unit-area runoff (q) and soil loss (SL) at different spatial scales (microplot: 1 m^2, plot: 10 m^2, microcatchment: 0.23 km^2, subcatchment: 1.20 km^2, catchment: 9.75 km^2, sub-basin: 253 km^2, and basin: 29,038 km^2) in Thukela basin during the study period.

	2010–2011	2011–2012	2012–2013	2013–2014	Mean
q (L m^{-2} yr^{-1})					
1 m^2	539	273	343	320	**369**
10 m^2	434	218	272	269	**298**
0.23 km^2	714	258	309	327	**402**
1.20 km^2	163	67	103	47	**95**
9.75 km^2	0.04	0.03	0.04	0.04	**0.04**
253 km^2	Nd	nd	nd	73	**73**
29,038 km^2	0.1	0.08	0.08	0.14	**0.1**
SL (g m^{-2} yr^{-1})					
1 m^2	3619	1608	1889	1803	**2230**
10 m^2	3646	1704	1853	1847	**2263**
0.23 km^2	316	182	337	389	**306**
1.20 km^2	57	6	13	4	**20**
9.75 km^2	4×10^{-4}	2×10^{-4}	0.28	0.29	**0.14**
253 km^2	Nd	nd	nd	0.06	**0.06**
29,038 km^2	Nd	nd	nd	nd	**nd**

nd not determined.
The bold values in Table 2 are annual average values for the four year study period.

from microplot to plot scales (Table 1; Fig. 3b–c) has also been observed at other hillslopes (e.g. Le Bissonnais et al., 1998; Parsons et al., 2006) and can be explained in terms of evolving erosion mechanisms. Soil erosion at microplots is dominated by the transport limited splash mechanism; while the longer slope at plot level enables flow velocities to mobilize adequate energy for lateral sheet wash. Therefore, sheet wash tends to be more competent than splash in terms of transportation of detached materials. However, the soil losses increase with slope length up to a peak before declining with further increase in slope length (Kinnell, 2009). The location of peak point varies with slope gradient, rainfall intensity and infiltrations conditions amongst many factors. On our study slope, the peak point is likely to be at a slope length greater than 5 m. The reduction of unit-area soil losses with further increase of area on hillslopes signifies redistribution of sediments within the slopes and deposition at footslopes (Chaplot et al., 2005). In our study, sediment concentrations and soil loss fluxes were much lower at microcatchment than local scales despite evidence of the operation of more erosive mechanisms (e.g. sheet, gully and stream bank erosion). Such results can be explained by greater heterogeneity and variability of landscape features (e.g. slope, basal cover, complexity of erosion processes like increased detachment, transport and deposition cycles) at microcatchment than local scales which favoured greater sedimentation. The same appeared to occur at subcatchment level, where sediment fluxes were even lower. Several studies have also shown lower unit-area runoff and sediment fluxes on stream channels than hillslopes (Constantz, 1998; Feng and Li, 2008; Goransson et al., 2013; Xu, 2014) due to lower slope gradients which promote high infiltration and sediment deposition (Doble et al., 2012; Eder et al., 2014).

Results of cumulative runoff (Table 2) showed great annual runoff microcatchment level, which in some years (e.g. 2010–2011 and 2013–2014) was greater than at microplot level. High microcatchment level annual runoff has also been reported at this station by other studies (Chaplot and Ribolzi, 2014; Orchard et al., 2013) and at other footslopes (e.g. Castro dos Reis et al., 1999; Uhlenbrook et al., 2005; Van Tol et al., 2013). The main reason proffered by the other studies is downslope movement of soil water and exfiltration to join overland flow systems at footslopes and stream channels. The results of annual unit-area runoff in our study also suggest the existence of an annual rainfall threshold (of about 800 mm yr^{-1}) above which cumulative runoff at microcatchment would be greater than at microplot level. Number of rain-days and days of high intensity rainfall can explain this result. The years 2010–2011 and 2013–2014 (rainfall > 800 mm yr^{-1}) had greater number of rain-days and incidences of greater than 20 mm day^{-1} rainfalls than 2011–2012 and 2012–2013 (<800 mm year^{-1}). Coincidentally, 2010–2011 and 2013–2014 had greater cumulative runoff at microcatchment than microplot level, and opposite in 2011–2012 and 2012–2013.

The results showing decline of correlation coefficients between rainfall characteristics and fluxes with scale size (Table 3) suggest rainfall effect on the fluxes was a local phenomenon whose significance would diminish with landscape area. This agrees with findings by Chamizo et al. (2012) who identified rainfall characteristics as major proponents of runoff generation at local scale only. Indices for rainfall amount (i.e. Rainfall and Dur) appeared to have greatest effect on the fluxes, followed by rainfall intensity indices (I and $Max_{6min}I$) and lastly the moisture indices (Prerain-3 and RainC) at all headwater scales during the study. However, other environmental parameters need to be appraised.

Table 3
Spearman rank correlations between headwater rainfall characteristics (Rainfall: total rainfall amount per day, Dur: total duration of rainfall events per day, I: average rainfall intensity in a day, $Max_{6min}I$: maximum 6-min rainfall intensity in a day, PreRain-3: antecedent 3-day rainfall and RainC: cumulative rainfall since the onset of the main rain season) and fluxes (q: unit-area runoff, SC: sediment concentration and SL: soil loss) at different scales (microplot: 1 m^2; plot: 10 m^2, microcatchment: 0.23 km^2, subcatchment: 1.20 km^2, and catchment: 9.75 km^2) in the headwater of Thukela basin.

		Rainfall characteristics					
Fluxes	Spatial scale	Rainfall (mm day^{-1})	Dur (mins)	I (mm h^{-1})	$Max_{6min}I$ (mm h^{-1})	PreRain-3 (mm)	RainC (mm)
q (L m^{-2} day^{-1})	1 m^2	0.80*	0.80*	0.71*	0.71*	0.66*	0.19*
	10 m^2	0.80*	0.80*	0.71*	0.71*	0.66*	0.19*
	0.23 km^2	0.57*	0.57*	0.55*	0.55*	0.57*	0.54*
	1.20 km^2	0.26*	0.26*	0.26*	0.26*	0.31*	0.44*
	9.75 km^2	−0.02	−0.02	−0.01	−0.01	0.00	0.36*
SC (g L^{-1})	1 m^2	0.79*	0.79*	0.71*	0.71*	0.66*	0.19*
	10 m^2	0.79*	0.79*	0.71*	0.71*	0.66*	0.19*
	0.23 km^2	0.52*	0.51*	0.46*	0.46*	0.30*	0.12*
	1.20 km^2	0.45*	0.45*	0.41*	0.41*	0.28*	0.13*
	9.75 km^2	0.44*	0.44*	0.40*	0.40*	0.28*	0.15*
SL (g m^{-2} day^{-1})	1 m^2	0.80*	0.80*	0.71*	0.71*	0.66*	0.19*
	10 m^2	0.80*	0.80*	0.71*	0.71*	0.66*	0.19*
	0.23 km^2	0.61*	0.61*	0.58*	0.58*	0.57*	0.53*
	1.20 km^2	0.35*	0.35*	0.34*	0.34*	0.35*	0.44*
	9.75 km^2	0.12*	0.12*	0.11*	0.11*	0.07*	0.35*

*Significant at $p < 0.05$.

5. Conclusions

The objectives of this study conducted in Thukela Basin, South Africa, were to (i) evaluate water and sediment fluxes at different spatio-temporal scales, and (ii) interpret the results in terms of processes involved and factors of control. The results showed a decrease of unit-area runoff by 2.6 fold from microplot to plot scales followed by a sharp decrease at the o microcatchment level. Unit-area runoff decreased in downstream direction to very low values. Different soil erosion mechanisms, dependent on spatio-temporal scales, accompanied the changes in unit-area runoff culminating in 1% increase of average unit-area soil loss from microplot to plot scale and a very sharp (39 fold) decline at the microcatchment scale. The soil loss fluxes also decreased to very low values in the downstream direction. The change in sediment fluxes was associated with evolution of soil erosion types, from lateral to linear mechanisms. Splash erosion dominated at micro-plot scale, changing to the more transport competent lateral sheet erosion mechanism at plot scale. However, despite evidence of the operation of linear erosion mechanisms at microcatchment scale and beyond sediment fluxes were very low on the stream channel due to deposition on the slope and stream channel. In order to mitigate soil erosion at the study site, strategies to promote the recovery of vegetation and stabilisation of gullies are recommended.

Acknowledgements

The research leading to these results has received funding from the European Community's Seventh Framework Programme (FP7/2007–2013) under the WHaTeR project (Water Harvesting Technologies Revisited) grant agreement n^{o} 266360, Water Research Commission (WRC K5/2266) and African Conservation Trust (ACT).

References

Asadzadeh, F., Gorji, M., Vaezi, A., Sokouti, R., Shorafa, M., 2012. Scale effect on runoff from field plots under natural rainfall. Am. Eur. J. Agric. Environ. Sci. 12 (9), 1148–1152.
Cammeraat, E.L.H., 2004. Scale dependent thresholds in hydrological and erosion response of a semi-arid catchment in southeast Spain. Agric. Ecosyst. Environ. 104, 317–332.
Castro dos Reis, N.M., Auzet, A.V., Chavellier, P., 1999. Land use change effect on runoff and erosion from plot to catchment scale on the basaltic plateau of Southern Brazil. Hydrol. Process 13, 1621–1628.
Chamizo, S., Canton, Y., Rodriguez-Caballero, E., Domingo, F., Escudero, A., 2012. Runoff at contrasting scales in a semi-arid ecosystem: a complex balance between biological soil crust features and rainfall characteristics. J. Hydrol. 452–453, 130–138.
Chaplot, V.A.M., Rumpel, C., Valentin, C., 2005. Water erosion impacts on soil and carbon redistribution within uplands of the Mekong basin. Glob. Biogeochem. Cycles 19, 20–32.
Chaplot, V., Ribolzi, O., 2014. Hydrograph separation to improve understanding of dissolved organic carbon dynamics in headwater catchments. Hydrol. Process 28, 5354–5366.
Chihombori, J., Nyoni, K., Gamira, D., 2013. Causes and rate of reservoir sedimentation due to changes in catchment management: a case of Marah Dam in Masvingo Province of Zimbabwe. Greener J. Physic. Sci. 3 (6), 241–246.
Constantz, J., 1998. Interaction between stream temperature, stream flow, and ground water exchanges in alpine streams. Water Resour. Res. 34, 1609–1615.
Deckers, J.A., Nachtergaele, F.O., Spargaren, O.C. (Eds.), 1998. Introduction to World Reference Base for Soil Resources, first ed. ISSS. ISRC. FAO. Acco, Leuven, Belgium.
De Vente, J., Poesen, J., 2005. Predicting soil erosion and sediment yield at the basin scale: scale issues and semi-quantitative models. Earth Sci. Rev. 71, 95–125.
De Vente, J., Poesen, J., Arabkhedri, M., Verstraeten, G., 2007. The sediment delivery problem revisited. Prog. Phys. Geogr. 31 (2), 155–178.
Dlamini, P., Orchard, C., Jewitt, G., Lorentz, S., Titshall, L., Chaplot, V., 2011. Controlling factors of sheet erosion under degraded grasslands in the sloping lands of KwaZulu-Natal, South Africa. Agric. Water Manag. 98, 1711–1718.
Doble, R., Brunner, P., McCallum, J., Cook, P.G., 2012. An analysis of river bank slope and unsaturated flow effects on bank storage. Groundwater 50 (1), 77–86.
Dunkerley, D., 2010. Ecogeomorphology in the Australian drylands and the role of biota in mediating the effects of climate change on landscape processes and evolution. In: Bishop, P., Pillans, B. (Eds.), Australian Landscapes, vol. 346. Geol. Soc., London, Special Publications, pp. 87–120.
Eder, A., Exner-Kittridge, M., Strauss, P., Blöschl, G., 2014. Re-suspension of bed sediment in a small stream – results from two flushing experiments. Hydrol. Earth Syst. Sci. 18, 1043–1052.
Feng, P., Li, J.Z., 2008. Scale effects on runoff generation in meso-scale and large scale sub-basins in the Luanhe River basin. Hydrol. Earth Syst. Sci. Discuss. 5, 1511–1531.
Flugel, W., Marker, M., Moretti, S., Rodolfi, G., Sidrochuk, A., 2003. Integrating geographical information systems, remote sensing, ground trothing and modelling approaches for regional erosion classification of semi-arid catchments in South Africa. Hydrol. Process 17, 929–942.
Goransson, G., Larson, M., Bendz, D., 2013. Variation in turbidity with precipitation and flow in a regulated river system-river Gota Alv, SW Sweden. Hydrol. Earth Syst. Sci. 17, 2529–2542.
Joel, A., Messing, I., Seguel, O., Casanova, M., 2002. Measurement of surface water runoff from plots of two different sizes. Hydrol. Process 16, 1467–1478.
Kinnell, P.I.A., 2008. Sediment delivery from hillslopes and the universal soil loss equation: some perceptions and misconceptions. Hydrol. Process 22, 3168–3175.
Kinnell, P.I.A., 2009. The impact of slope length on the discharge of sediment by rain impact saltation and suspension. Earth Surf. Process. Landf. 34, 1393–1407.
Kongo, V.M., Kosgei, J.R., Jewitt, G.P.W., Lorentz, S.A., 2010. Establishment of a catchment monitoring network through a participatory approach in a rural community in South Africa. Hydrol. Earth Syst. Sci. 14, 2507–2525.
Lal, R., 2004. Soil carbon sequestration impacts on global climate change and food security. Science 304 (5477), 1623–1627.
Le Bissonnais, Y., Benkhadra, H., Chaplot, V., Fox, D., King, D., Daroussin, J., 1998. Crusting, runoff and sheet erosion on silty loamy soils at various scales and upscaling from m2 to small catchments. Soil Till. Res. 46, 69–80.
Mayor, A.G., Bautista, S., Bellot, J., 2011. Scale-dependent variation in runoff and sediment yield in a semiarid Mediterranean catchment. J. Hydrol. 397, 128–135.
Négrel, P., Merly, C., Gourcy, L., Cerdan, O., Petelet-Giraud, E., Kralik, M., Klaver, G., van Wirdum, G., Vegter, J., 2014. Soil-sediment-river connections: catchment processes delivering pressures to river catchments. In: Brils, J., Brack, W., Muller-Grabherr, D., Négrel, P., Vermaat, J.E. (Eds.), Risk-informed Management of European River Basins, the Handbook of Environmental Chemistry, p. 29. http://dx.doi.org/10.1007/978-3-642-38598-8_2.
Oakes, E.G.M., Hughes, J.C., Jewitt, G.P.W., Lorentz, S.A., Chaplot, V., 2012. Controls on a scale explicit analysis of sheet erosion. Earth Surf. Process. Landf. 37, 847–854.
Orchard, C.M., Lorentz, S.A., Jewitt, G.P.W., Chaplot, V.A.M., 2013. Spatial and temporal variations of overland flow during rainfall events and in relation to catchment characteristics. Hydrol. Process 27, 2325–2338.
Parsons, A.J., Brazier, R.E., Wainwright, J., Powell, D.M., 2006. Scale relationships in hillslope runoff and erosion. Earth Surf. Process. Landf. 31, 1384–1393.
Schulze, R., 1997. South African Atlas of Agro Hydrology and Climatology. TT82/96. Water Research Commission, Pretoria, RSA.
Shi, Z.H., Fang, N.F., Wu, F.Z., Wang, L., Yue, B.J., Wu, G.L., 2012. Soil erosion processes and sediment sorting associated with transport mechanisms on steep slopes. J. Hydrol. 454–455, 123–130.
Smith, H.G., Dragovich, D., 2007. Sediment supply from small upland catchments: possible implications of headwater channel restoration for stream management. In: Wilson, A.L., Dehaan, R.L., Watts, R.J., Page, K.J., Bowmer, K.H., Curtis, A. (Eds.), Proceedings of the 5th Australian Stream Management Conference. Australian Rivers: Making a difference. Charles Sturt University, Thurgoona, New South Wales.
Sorman, A.U., Abdulrazzak, M.J., 1993. Infiltration-recharge through wadi beds in arid regions. Hydrol. Sci. J. 38 (3), 173–186.
Thomaz, E.L., Vestena, L.R., 2012. Measurement of runoff and soil loss from two differently sized plots in a subtropical environment (Brazil). Earth Surf. Process. Landf. 37, 363–373.
Uhlenbrook, S., Wenninger, J., Lorentz, S., 2005. What happens after the catchment caught the storm? Hydrological processes at the small, semi-arid Weatherly catchment, South Africa. Adv. Geosci. 2, 237–241.
Van de Giesen, N.C., Stomph, T.J., de Ridder, N., 2000. Scale effect of Hortonian overland flow and rainfall-runoff dynamics in a West African catena landscape. Hydrol. Process 14, 165–175.
Van Tol, J.J., Le Roux, P.A.L., Lorentz, S.A., Hensely, M., 2013. Hydropedological classification of south african hillslopes. Vadose Zone J. 12 (4) doi: 10.213/vzj2013.01.0007.
Xu, J., 2014. Decreasing trend of sediment transferring function of the upper Yellow River, China, in response to human activity. Hydrol. Sci. J. http://dx.doi.org/10.1080/02626667.2014, 885655.

Please cite this article in press as: Mutema, M., et al., Spatial scale impact on daily surface water and sediment fluxes in Thukela river, South Africa, Physics and Chemistry of the Earth (2015), http://dx.doi.org/10.1016/j.pce.2015.10.001